Increased scale and accessibility of sediment transport research in rivers through practical, open-source turbidity and depth sensors

Theodore Langhorst (tlang@live.unc.edu)
University of North Carolina at Chapel Hill https://orcid.org/0000-0003-0366-4809
Tamlin Pavelsky
University of North Carolina
Emily Eidam
Oregon State University
Lillian Cooper
University of North Carolina at Chapel Hill
Julianne Davis
University of North Carolina at Chapel Hill
Katie Spellman
University of Alaska Fairbanks https://orcid.org/0000-0002-2291-0190
Sarah Clement
University of Alaska Fairbanks
Christopher Arp
University of Alaska Fairbanks
Allen Bondurant
University of Alaska Fairbanks
Elisa Friedmann
University of Massachusetts at Amherst
Colin Gleason
University of Massachusetts at Amherst

Article

Keywords:

Posted Date: April 18th, 2023

DOI: https://doi.org/10.21203/rs.3.rs-2793579/v1

Version of Record: A version of this preprint was published at Nature Water on September 4th, 2023. See the published version at https://doi.org/10.1038/s44221-023-00124-2.

Abstract

Open-source designs for turbidity and depth sensors are becoming increasingly capable and available, but the knowledge required to construct them limits their use compared to expensive, commercial sensors. Here, we present an open-source optical backscatter and water pressure sensor that can be ordered almost fully assembled, requires no coding to deploy, and costs approximately $50 USD. We share three examples of these sensors' ability to facilitate new research. First, we observed complex changes in spatial and temporal patterns of suspended sediment transport in the Arctic Sagavanirktok River using a network of sensors. Second, we measured turbidity during the freeze-up period in the Tanana River, a period of high risk to sensors. Last, we built and deployed sensors with middle-school students to monitor turbidity under full ice cover on the Tanana River. The success of open-source sensors in these examples shows a marked increase in scale and accessibility of river science.

Introduction

Measurements of turbidity and water depth are key components of monitoring the suspended sediment transport of a river. The concentration of suspended solids in the water column can be calibrated to turbidity with in-situ measurements or lab resuspensions[1], and discharge can be calibrated to river depth using a rating curve developed from hydraulic geometry[2]. The product of suspended solids and discharge produces a simple estimation of the total suspended sediment flux[3]. A river's sediment flux often varies on a daily scale as the watershed experiences changing precipitation, temperatures, and antecedent conditions[4]. Sediment flux can also vary over longer timescales. For example, rivers in glaciated basins can transport nearly half of their annual sediment flux during the spring snowmelt period[5,6]. The unique factors controlling the timing of sediment flux in different watersheds necessitate monitoring over long periods to accurately characterize riverine sediment transport. Extending this principle beyond a single point measurement to observe the complex spatial and temporal patterns of sediment moving through an entire watershed requires an extensive network of sediment flux observations[7].

Field-deployable commercial turbidity and pressure sensors cost upwards of $3000 USD, which constrains our ability to measure and study complex patterns of river sediment transport. Research projects that are not well-funded may be unable to secure commercial sensors, while well-funded research will use these sensors conservatively due to the risk of loss. Among many other systemic injustices in the geoscience community, non-white principal investigators are less frequently funded by the National Science Foundation than their white colleagues [8] . Reducing the barriers for access to laboratory equipment has been shown to increase engagement with undergraduate, graduate, women, and non-U.S. scientists above geoscience norms [9] . By definition, open-source sensors are available to anyone and are typically less expensive than commercial options, but their measurement quality and usability often limit widespread application. Better, more-developed open-source sensors therefore have the potential to facilitate large-scale, high-risk studies, and improve the accessibility of scientific instrumentation. Open-source sensor designs are becoming increasingly popular, illustrated by sensor

publications increasing by an order of magnitude over the past decade [10] . Unfortunately, this popularity is primarily reflected in engineering, computer science, instrumentation, and other technology-focused journals, and is only beginning to emerge in the natural sciences [10] . Even within the environmental monitoring subset of open-source sensors, a focus on technology development leads to publications that describe soldering, embedded programming, and the virtues of open source technology, rather than presenting scientific applications [11] . While the low-cost of open-source sensors dismantles some barriers to science, compared to commercial sensors, do-it-yourself sensors have additional barriers in regards to:

- required knowledge of electronics
- accuracy and calibration
- ease of deployment

Here, we present the OpenOBS-328 as a further refinement of the OpenOBS project[12], improving on the three design principles above. The custom circuit board of the sensor can be completely manufactured by electronics assembly companies, leaving only the sensor head for the user to assemble. The turbidity sensor response is highly linear ($R^2 > 0.999$) over a range of 0-1000 NTU (and likely beyond), meaning calibration can be achieved with as few as 2 samples. The pressure sensor comes calibrated from the factory for up to 14 bars of pressure (~ 130 m water depth) and with an accuracy of less than 0.2 mbar (~ 0.2 cm of water). To address the ease of use, we developed a graphical user interface for deploying the sensors that updates the time and measurement settings. Other open-source sensors typically rely on advanced knowledge of embedded electronics, which was already required for assembly, and have users edit code and upload new sensor firmware before deploying.

The OpenOBS has already enabled science with denser sampling and higher risk tolerance than possible with commercial sensors. While most open-source turbidity sensors have been tested in the lab or in limited, short-term field contexts, we have built more than 90 OpenOBSs and deployed them around the world. To our knowledge, OpenOBSs have been deployed in coastal estuaries and rivers of North Carolina, California, and Alaska, USA, as well as rivers in Greenland, Chile, and Nepal. We present results from three such deployments, in the Sagavanirktok and Tanana Rivers, to illustrate the use of these sensors to address science questions that would otherwise require placing thousands of dollars of commercial sensors at significant risk. In our third example, middle school students built sixteen sensors to study under-ice turbidity and ambient light conditions, which highlights the increased access and learning opportunities provided by open-source sensors.

Main Text

This sensor development and work on the Tanana River was supported by NSF grant 2153778 (PI Emily Eidam). The data collection on the Sagavanirktok River was supported by The Preston Jones and Mary Elizabeth Frances Dean Martin Trust Fund in the Department of Earth, Marine and Environmental Sciences at the University of North Carolina at Chapel Hill and NSF grant 1748653 (PI Colin Gleason).

1. Turbidity Sensors

Turbidity is a measurement of the optical clarity of water. Water clarity affects the penetration of light through the water column and is impacted by scattering and absorption as a result of both dissolved and particulate matter. Light penetration in turn impacts available energy for ecological and biogeochemical processes [13,14] . We often relate turbidity to suspended sediment concentration (SSC) to monitor the flux of sediment through a river. Optical turbidity sensors measure the clarity of water by shining light into a sample and measuring either how much light passes through (transmissometer) or is scattered by (nephelometer, backscatter sensor) the sample volume. The exact optical properties of sediment change based on the grain size, shape, and reflectivity at the wavelength of the turbidity sensor. The measurements rely on the principle that water is optically dark in the near-infrared wavelengths (~ 750–1000 nm) and suspended particles are bright at the same wavelengths. The response of an optical backscatter sensor (OBS) is positively correlated with SSC, whereas the response of a transmissometer sensor is negatively correlated with SSC. Standalone, commercial turbidity sensors for field deployments cost at least $3000 USD.

The OpenOBS project developed the first field-deployable open-source turbidity sensor with a wide range of linear response to sediment concentration[12]. The OpenOBS closely matches the design of commercial sensors by using a reverse-biased photodiode and transimpedance amplifier to give a linear response across a wide range of suspended sediment concentration values[15] (up to 5 g/L). Other open source turbidity loggers had been developed previously, but they all either: used a phototransistor in their active region[16,17], which is only approximately linear for a small range compared to photodiode sensors; were designed for high resolution monitoring of low turbidity water[18,19]; or were designed for benchtop work in a laboratory[20]. Table 1 lists all published open-source turbidity sensors that have been tested in field deployments that we found in the literature. It is clear from Table 1 that there is a desire for low-cost, open-source turbidity sensors for research and environmental management, but the adoption and widespread use of these sensors is still limited.

Table 1
Comparison of optical, open source, in situ turbidity sensors.

Reference	Measurement angle (degrees)	Sensor type	Reported range (NTU)	Cost
Murphy et al., 2014[19]	90, 0	Photodiode	0–55	650 Euro
Kirkey et al., 2018[21]	120	Photodiode	0-815	70 USD
Matos et al., 2019[16]	135, 90, 0	Phototransistor	0-1000	20 Euro
Trevathan et al., 2020[17]	0	Phototransistor	100–4000	Not listed
Jiang et al., 2020[18]	90, 0	Photodiode	0–20	40 USD
Eidam et al., 2022[12]	180	Photodiode	0-1000	150 USD
Kinar & Brinkman, 2022[22]	0	Phototransistor	0-850	1000* CAD
Droujko & Molnar, 2022[23]	135, 90, 0	Photodiode	0-4000	61 CHF
Sanchez et al., 2023[24]	90, 0	Photodiode	0–50	50 USD
Droujko et al., 2023[25]	135	Photodiode	0-500	200* Euro
OpenOBS-328	180	Photodiode	0-1000	50* USD

*Includes other sensors

Costs are as reported in the publications. Authors took varied approaches to cost reporting including amortizing equipment and consumables, labor, or calibration materials. Similarly, the reported range reflects what the manuscript deemed as the usable range, and we did not make judgements on the accuracy of the sensors. A measurement angle of 0 represents a transmissometer, where the detector is directly facing the emitter. A measurement angle of 180 represents a backscatter sensor, where the detector and emitter face the same direction.

2. Depth Sensors

There are a variety of popular methods for measuring water depth including: staff gages, stilling wells, echo-sounders, and pressure transducers. The last option, pressure transducers, are compact, affordable, and convenient for temporary installation in most environments. Commercial loggers cost around $400 USD and provide centimeter accuracy. Open-source designs for water depth sensors are also prevalent in

the literature and have seen more widespread adoption than turbidity sensors [11, 25–29] . Unlike the variety of custom designs used to measure turbidity by the devices in Table 1, these open-source depth sensors all use the MS5803 pressure sensor by TE Connectivity. This sensor is cost-effective and is highly accurate. The MS5803 is an absolute pressure sensor, meaning it is referenced to a vacuum, and water depth measurements need to be corrected for changes in atmospheric pressure.

3. **Applications**

A. High-resolution Monitoring

We installed 10 OpenOBS loggers at 5 locations (2 per location) along a 35 km section of the Sagavanirktok River, Alaska in June 2022 (Fig. 2a). At each site, we measured turbidity, pressure, and water temperature hourly until the loggers were removed in late August. During this period, we observed several pulses of high discharge and turbidity, and our dense network of sensors allowed us to observe these events over the length of the river. Over the 3-month deployment we observed sediment transport patterns changing from the snowmelt-dominated early summer to the flashy rain events that dominate the mid and late summer (Fig. 2b and 3c). After snowmelt, the high-energy flow in the mountain headwaters quickly flushes the available sediment, whereas the tundra watershed and banks are still mostly frozen and highly resistive. In mid-summer, after the snowmelt period, we saw a consistent decrease in the turbidity as the sediment wave traveled downstream, likely a result of dilution by small tributaries that add clear water to the Sagavanirktok between our sites. In late summer, we see increasing turbidity downstream, suggesting the addition of sediment to the main channel from the banks and the small tributaries. By late summer, the mountains are exhausted of entrainable sediment, and a greater component of the total sediment is likely sourced from the recently-thawed banks and active layer near our sites.

The high temporal resolution of our loggers, compared to data from bottle sampling or remote sensing, allows us to investigate the difference in the time of peak water level and peak TSS at each location. The time lag between sediment concentration and water level (hysteresis) relates to the sediment source for that event. Over the course of the summer, we see distinct changes in the hysteresis on the Sagavanirktok. In the early summer period, we see multiple flow and sediment signatures imprinted on the hysteresis plot. Over the full 60 hours we see clockwise movement, with higher water levels for the same turbidity values at the end of the period. There is also a clear diurnal pattern because runoff from snowmelt is the greatest component of river discharge in the early summer (also seen in Figs. 2b and 2c). The area defined by each daily hysteresis loop is much smaller than later in the season and the patterns are more irregular. Two of the daily hysteresis loops are counterclockwise, while the middle loop forms a figure eight pattern that is ultimately clockwise at the peak. In mid-summer we see the discharge wave precede the sediment wave (counterclockwise hysteresis). This pattern can indicate that the sediment source is relatively farther from the monitoring site, or the sediment is a result of bank failure during the falling water levels[4]. In late summer, we see hysteresis in the opposite direction (clockwise hysteresis),

which typically occurs when the sediment source is close to the monitoring site or is exhausted quickly by the increased transport capacity of the discharge wave. Similar shifts in hysteresis as a result of changing water and sediment sources have been observed in several other studies of Arctic rivers[5,30,31]

In this example, the low-cost OpenOBS loggers allowed us to observe complex suspended transport patterns on an Arctic river with high spatial and temporal resolution for less than the cost of one commercial turbidity sensor. Without access to these sensors, our budget would have limited the research to a single commercial sensor during the three weeks we were on site, rather than duplicated measurements at five locations for nearly three months.

B. High-risk Environment Monitoring

When we install any sensor in a river, we risk losing it due to heavy sedimentation, floating woody debris, high flows, ice, vandalism, or any number of environmental and human factors. We deployed three OpenOBS sensors in the Tanana River, Alaska in October 2022 to monitor sediment transport during freeze up and ice-covered periods. This period is difficult to monitor, with regards to both personnel safety and risk to sensors, because of weather and ice hazards. A drop in temperature and low water levels can freeze sensors in place or make them otherwise inaccessible by boat, trapping sensors in the river for the duration of the winter until ice breakup. We were able to accept these risks because of the relatively low cost of our sensors and the ability to back up the data in real time via satellite transmission.

We attached sensors to Iridium-equipped loggers (described in Methods 1d) which transmitted data to us every 3 hours, ensuring we would receive data even if the loggers were damaged later in the winter. One of our three sensors was deployed in a relatively shallow portion of the river that froze solid and stopped transmitting meaningful data. A second sensor was deployed in an active part of the channel that showed a high concentration of frazil ice when we drilled through the thick layer of ice in December and January. Unfortunately, ice and sediment are both highly reflective in the near-infrared wavelengths, and we suspect the presence of ice suspended in the water column starting in mid-October caused an increase in the backscatter values (Fig. 3). Nevertheless, we were able to monitor turbidity, water level, and temperature in the Tanana River in late fall without worrying about retrieving our sensors before they froze in for the winter. While all three sensors were operational, we observed a sediment wave passing through this section of the Tanana River. On the descending limb of the data from each site, there are occasional small increases in turbidity, which may represent bank collapses or other more local sediment mobilization from the bed, banks, or bars.

C. Accessibility

Low cost sensors provide opportunities for research and environmental monitoring that are not funded by large research grants. In our experience with the original OpenOBS, student research projects have benefited greatly from open-source sensors. The OpenOBS itself started as an undergraduate research

project and was continued over several years for graduate research on the Sagavanirktok River (Section 3a) and an NSF-funded multi-institutional study of the Tanana River (Section 3b). Over the past three years, one graduate and two undergraduate projects at the University of North Carolina at Chapel Hill have used the OpenOBS loggers to monitor sediment transport in coastal North Carolina[32].

We have also used the OpenOBS design to teach middle school students about rivers, sediment, and the scientific process. We discussed the students' perspectives on sediment in rivers, with some focus on how it affects sunlight in the water. Although the OpenOBS uses invisible near-infrared light, the principle that light penetrates clear water and reflects or scatters off of particles in the water is common to both the principle of turbidity measurements and our visual experiences with rivers. Thirty-nine students from the Nenana City School in Nenana, Alaska and the CyberLynx homeschool program in Fairbanks, Alaska hand soldered 16 sensors (Fig. 4a). The students developed hypotheses regarding where the sediment would be highest or lowest within a river reach and decided where they wanted to take their measurements. We deployed four of their sensors (and two that we built and calibrated) through the ice (Fig. 4b, 4c) to address the class hypotheses.

After approximately one month of data collection, we retrieved the sensors and analyzed the data. The three sensors in Nenana all experienced some degree of biofouling. Of the three sensors installed near Fairbanks, one fell out of the mounting device and was lost, one showed occasional high backscatter likely due to ice, and the final sensor experienced a 3-day period of missing data. While these issues alone were a lesson on the reality of the scientific process (not specific to open-source or commercial sensors), we also recovered some usable data (Fig. 4d). Turbidity in the Tanana River in late January, with thick ice cover and low flows, is unsurprisingly low (approximately 5 NTU). The ambient light readings show a low but observable level of visible light penetration through the thick snow and ice cover. In this example, the do-it-yourself aspect of the sensor construction provided an opportunity to engage with students. The low-cost aspect of the sensor allowed us to build and deploy several sensors with student-led science objectives.

Conclusions

Open-source sensors have the potential to ease the financial burden associated with purchasing commercial sensors for researchers. The barriers to do-it-yourself sensors are high in other ways, primarily in the knowledge and equipment required to build and operate them. We developed the OpenOBS-328 to use the same measurement principles as commercial sensors, resulting in similar accuracy. Equally importantly, we developed OpenOBS-328 to the point that it can be easily constructed and used by geoscience researchers without experience in electronics. The device can be ordered from online manufacturers almost completely assembled, requiring no more than two hours of labor to have a fully operational and calibrated sensor. Field scientists deploying the sensor only need to download a graphical user interface to program the deployment settings or update the firmware (Figure S6).

Since the development of the OpenOBS in 2019, we have constructed more than 90 sensors and installed them in rivers from coastal North Carolina to the North Slope of Alaska. Collaborators have used the sensors to enable research in Chile, Greenland, Nepal, and California, USA. The three examples shown here (all in Alaska) demonstrate the capability of the sensor to monitor suspended sediment flux accurately and reliably for scientific research. Additionally, two undergraduate research projects at the University of North Carolina at Chapel Hill have been enabled by the affordability of these sensors. Two classes of middle school students built 16 OpenOBS sensors, developed hypotheses about sediment in the Tanana River, and deployed sensors through the ice in January. With the further development of the OpenOBS project presented here, the sensor is now more capable and easier to assemble. While we hope the OpenOBS-328 will continue to evolve and improve in the future, we have shown that the sensor has already grown beyond a do-it-yourself electronics project into a practical instrument for sediment transport research.

Methods

1. **OpenOBS-328 design**

A. Sensor

The OpenOBS-328 is designed to use the VCNL4010 proximity sensor calibrated for turbidity. In contrast to the original OpenOBS design, which included a discrete photodiode and transimpedance amplifier, the VCNL4010 is a fully integrated solution that handles all of the optical sensing, amplification, and analog-to-digital conversion (Fig. 1b). The VCNL4010 is designed for relative distance measurements (for example, detecting a hand under a soap dispenser) but uses the same measurement principles as optical backscatter sensors for turbidity:

● An infrared light emitting diode (IRED) is pulsed between 0 and 50 mA at 390 kHz. This IRED has a peak emission wavelength of 890 nm. The IRED has a flat lens, giving it a wide angle and nearly Lambertian emission distribution, which has the effect of measuring the entire sampling volume equally.

● One photo-pin-diode (PD) senses the infrared light scattered by particles in the water during the ‘on’ phase of the IRED. There is an optical filter that reduces all light below 800 nm, and the PD has a peak sensitivity at 880 nm. During the ‘off’ phase of the IRED, the PD senses the background infrared light for an offset correction.

● A second PD senses the visible ambient light conditions. The ambient light PD is sensitive to wavelengths from 400 to 700 nm with a peak sensitivity at 550 nm. This spectrum covers the same range as photosynthetically active radiation measurements, but the peak sensitivity at 550 nm makes the sensor unsuitable for true photosynthetically active radiation measurements.

The OpenOBS-328 is also able to measure changes in water level using the MS5803 pressure sensor (Fig. 1c). Similar to the VCNL4010, the MS5803 is a fully integrated sensor that handles both the analog sensing and the analog-to-digital conversion. We use the 5 and 14 bar maximum pressure variants of the MS5803, which translates to maximum depths of approximately 40 and 130 meters, respectively. Despite the wide range of measurement, the 24-bit analog to digital converter has a resolution of 0.2 mbar and an accuracy of 1.5 mbar (0.2 cm and 1.5 cm water depth, respectively). The MS5803 uses a piezoresistive sensor in a Wheatstone bridge configuration to measure pressure, and is factory calibrated. Each sensor's correction factors are stored in memory and are used in converting the raw sensor response to units of pressure.

Both sensors communicate using a 4-wire I2C communication protocol. The I2C communication bus allows multiple devices to be connected and individually addressed, which means anyone can add new I2C sensors to the OpenOBS-328 without modifying the electronics design. The OpenOBS-328 I2C bus operates at a maximum of 3.3V and connects to the logger using a qwiic connector (https://www.sparkfun.com/qwiic; 4-pin JST-SH).

B. Logger

The OpenOBS-328 data logging circuit board builds upon the original OpenOBS with some minor refinements in the functionality and major improvements to size and manufacturability. The module-based design of the OpenOBS developed naturally from the prototype stage of the project using readily available parts. The downsides of the old design are the relatively large size of the parts, manual soldering of the modules, and expense of the components. While the schematic of the OpenOBS was based on connecting "modules" that each perform a specific task, the OpenOBS-328 schematic (Figure S1) builds the functionality of each module onto one custom circuit board (Fig. 1a). The new "-328" suffix is a reference to the ATmega328p microprocessor that is used to control the circuitry.

There are existing open source data loggers that include the same basic functions and could interface with the same sensors we use; however, a custom design allows us to fit the sensor in a 1 inch PVC housing and reduce the power consumption. In between measurements, the voltage regulator that powers the sensor is turned off, and the only current draw is from the DS3231 real time clock and the power switching logic controls. When the real time clock reaches the programmed alarm time, the voltage regulator is enabled, and the entire circuit turns back on.

C. Housing

The extreme low-power consumption of the sensor also allows us to power the device with a single AA-size battery and design a small form-factor printed circuit board that fits inside a 1-inch diameter housing. We made a 3D-printed sensor head that holds the turbidity and pressure sensors at the end of the pipe. The turbidity sensor faces out perpendicular to the length of the long axis of the PVC pipe

(allowing for easy flush-mounting on instrument frames), the pressure sensor is embedded near the top, and both sensors are potted in epoxy to waterproof them (Fig. 1b and 1c). The epoxy for the turbidity sensor needs to be optically clear, so we mix a small amount of epoxy and then use a heat gun and a vacuum chamber to remove all bubbles. The pressure sensor does not require special properties of the epoxy, but the position of the sensor within the epoxy is critical to its function. The white pressure membrane on the top of the sensor must remain unaffected by epoxy while the bottom half of the sensor with electrical connections must be fully encased. After potting the sensors in the 3D printed head, this part is temporarily glued in the end of the PVC and then a layer of epoxy is poured inside for waterproofing. The opposite end of the housing is sealed with an expanding rubber plug. We tested the waterproof seal for the sensors by submerging them in water inside a pressure chamber and increasing the chamber pressure to simulate increased water depth. All three sensors remained dry for 48-hours at 43 PSI, equivalent to approximately 30 m water depth. We were unable to test at higher pressures to find a maximum depth, but open source sensors with similar construction have reported deployment up to 100 m[29].

D. Alternate Versions

We have developed two additional variations of the OpenOBS-328 to support our work. The first is a module-based design for educational outreach that is similar to the original OpenOBS (Section 4c). This version is more expensive and slightly less capable than the regular version, but it can be assembled by hand and is more easily understood because the modules provide a physical representation of each function of the logger. The schematics for the educational sensor are available in the supplemental (S3).

The second variation of our design allows the sensor to send data to us in real time from anywhere in the world using the Iridium network of satellites (Section 4b). Water interferes with the L-band Iridium communication frequency, so the sensor and logger components are physically separated by a data transmission cable. The sensor is deployed in the water connected to a logger installed onshore. The sensor does not have batteries or data storage inside but is otherwise similar to the autonomous version. Power is delivered to the sensor from the onshore logger, and the sensor sends data back to the logger using serial communications over a 4-wire cable. Because power and data are not located inside the sensor, we completely encase it in epoxy for extra durability. Transmitting data to the Iridium satellites requires substantially more power than the autonomous loggers; transmitting once per hour for a month uses 1400 mAh battery capacity at 3.7 V. As such, the Iridium deployments use larger, sealed lead-acid batteries and solar panels for power. The extra components of this version add approximately $500 USD to the total cost. The schematic for both sensor and logger of this version are also available in the supplemental (S4, S5).

2. OpenOBS-328 performance

A. Calibration

We individually calibrate each turbidity sensor after construction to account for inconsistencies in the sensor placement and epoxy clarity. We use tap water for our 0 NTU reference and 100, 250, 500, and 1000 NTU formazin standards for the other calibration points. We analyzed the calibration of the first 20 OpenOBS-328 sensors and found a highly linear (mean $R^2 > 0.999$) response to formazin standards. The residuals of a linear model have a standard deviation of 5.5 NTUs (3 standard deviations represent 1.65% of full scale; Fig. 6a). Commercial sensors report calibration accuracies of < 1–3% of full scale; however, intercomparisons of sensors reveal much higher disagreement[33,34]. These calibrations were used for the data presented in Figs. 2–5. An additional calibration between turbidity and SSC, or a single calibration directly from sensor response to SSC, will provide more useful data for estimates of suspended sediment flux.

The MS5803 pressure sensors we use are factory calibrated, so we do not calibrate them before deployment. However, the absolute pressure measured by the sensors needs to be converted to water depth using environmental variables. Calculating water depth from absolute pressure requires only a simple calculation (Eq. 1):

$$d = \frac{(P - P_A)}{(\rho * g)} \quad \text{Eqn. 1}$$

Where d is the water depth, P is the measured absolute pressure, P_A is the atmospheric pressure, ρ is the density of water, and g is the gravitational constant.

Atmospheric pressure is ideally measured by another instrument near the deployed sensor, but publicly available weather data can be substituted. The density of water primarily depends on salinity and temperature. We assumed zero salinity for our river applications and temperature was also measured by the MS5803, which is required to compensate for temperature drift in the piezoresistive elements.

B. Battery Life

The sensor functions in two modes to optimize battery life based on the measurement frequency. When the measurement interval is greater than 5 seconds, the entire logger is powered off except for the clock component that turns the power back on at a programmed time. We tested the battery consumption of the sensor using a Siglent 100 MHz oscilloscope and a 10 ohm shunt resistor in series with a 3.6V battery. The results were smoothed using a gaussian filter with a window of 2 ms to reduce high frequency noise (Figure S2). Each measurement takes approximately 0.96 seconds, and the average current consumption during the measurement is 10.8 mA. We do not have equipment that can accurately measure the sleep current between measurements, which is less than one tenth of a milliampere. Based on the datasheets for the real time clock and logic components that stay active during sleep, the only active components during sleep consume 22 µA. Leakage current through the components in the power circuit also contributes to this current, so we conservatively estimate the sleeping current at 50 µA (0.05mA). When the measurement interval is less than 5 seconds, waking the sensor from fully powered

off requires more energy than putting the logger in an idle state between measurements. We termed this ‘continuous mode’ because the logger never fully goes to sleep and measures at high frequency. In continuous mode the logger does not spend the extra time and power waking up and going to sleep, nor does the logger have to close and reopen the data file. Instead, the logger will take measurements at approximately 1 Hz and uses an average current of 2.0 mA (Figure S2). We estimate the battery life based on these current measurements, the measurement interval, and the battery capacity (equations 2, 3):

$$I = \frac{(10.8mA * 0.96s + 0.05mA * t_{off})}{(0.96s + t_{off})} \text{ for } t_{off} > 5s \quad \text{Eqn. 2}$$

$$I = 2.0mA \text{ for } t_{off} \leq 5s$$

$$T = \frac{I}{C} \quad \text{Eqn. 3}$$

Where I is the average current draw in mA, t_{off} is the time between measurements in seconds, C is the battery capacity in mAh, and T is the total battery life in hours.

We applied equations 2 and 3 for a range of measurement intervals from zero to 60 minutes for two different types of popular AA-size lithium batteries (Fig. 6b). With an 800 mAh rechargeable lithium-ion battery, the logger can run for a year at 4.1 minute logging intervals. With a 2000 mAh lithium thionyl chloride battery, the minimum interval to run for a year is 57 seconds. In continuous mode the two batteries would last 17 and 42 days respectively. Larger batteries or multiple batteries in parallel can be used for longer high frequency deployments. In reality, total battery capacity and leakage current depend on the temperature, average current draw, maximum pulse current, and many other factors that are difficult to control or predict. We estimated the battery capacity using conditions of 10°C and a constant 5mA discharge. Extremely long duration deployments also need to consider the self-discharge rate of batteries, which varies based on battery chemistry and temperature (colder temperatures decrease self discharge). Rechargeable lithium-ion batteries have self discharge rates of 0.25-3% per month, while lithium thionyl chloride batteries have significantly lower discharge rates of 0.25-4% per year.

Declarations

Availability statement

Github links will be archived in Zenodo before publication

Documentation for building, calibrating, using, and interpreting the OpenOBS-328 is available on our documentation site: https://tedlanghorst.github.io/OpenOBS-328/docs. All files and code for the sensor

design are available at the full repository path: https://github.com/tedlanghorst/OpenOBS-328.

The project is distributed with the GNU General Public License: https://www.gnu.org/licenses/gpl-3.0.en.html. Some of the libraries in the sensor firmware are modified from existing open-source projects and have retained other licenses, these are documented in the directory of each library.

Acknowledgements

We thank the students of the Nenana City School and their teacher, Braxtyn Gerald, as well as the CyberLynx students and their coordinator, Jill Stone, for their participation and help with building sensors. We also thank the Toolik Field Station staff, organized by Amanda Young, for their help retrieving our sensors from the Sagavanirktok River at the end of the 2022 summer season.

This sensor development and work on the Tanana River was supported by NSF grant 2153778 (PI Emily Eidam). The data collection on the Sagavanirktok River was supported by The Preston Jones and Mary Elizabeth Frances Dean Martin Trust Fund in the Department of Earth, Marine and Environmental Sciences at the University of North Carolina at Chapel Hill and NSF grant 1748653 (PI Colin Gleason).

References

1. Minella, J. P. G., Merten, G. H., Reichert, J. M. & Clarke, R. T. Estimating suspended sediment concentrations from turbidity measurements and the calibration problem. *Hydrol. Process.* **22**, 1819–1830 (2008).
2. Leopold, L. B. & Maddock, T. *The Hydraulic Geometry of Stream Channels and Some Physiographic Implications*. (1953).
3. Gray, J. R. & Simões, F. J. Estimating sediment discharge. in *Sedimentation Engineering: Processes, Measurements, Modeling, and Practice* (American Society of Civil Engineers, 2008). doi:10.1061/9780784408148.
4. Morehead, M. D., Syvitski, J. P., Hutton, E. W. H. & Peckham, S. D. Modeling the temporal variability in the flux of sediment from ungauged river basins. *Glob. Planet. Change* **39**, 95–110 (2003).
5. Chikita, K. A., Wada, T., Kudo, I. & Kim, Y. The Intra-Annual Variability of Discharge, Sediment Load and Chemical Flux from the Monitoring: The Yukon River, Alaska. *J. Water Resour. Prot.* **04**, 173–179 (2012).
6. Mao, L. & Carrillo, R. Temporal dynamics of suspended sediment transport in a glacierized Andean basin. *Geomorphology* **287**, 116–125 (2017).
7. Collins, A. L. & Walling, D. E. Documenting catchment suspended sediment sources: problems, approaches and prospects. *Prog. Phys. Geogr. Earth Environ.* **28**, 159–196 (2004).
8. Chen, C. Y. *et al.* Systemic racial disparities in funding rates at the National Science Foundation. *eLife* **11**, e83071 (2022).

9. Corbett, L. B., Bierman, P. R., Semken, S. & Whittaker, J. A. Can Community Laboratory Facilities Increase Access and Inclusivity in Geoscience? *Earth Space Sci.* **9**, e2021EA002028 (2022).
10. Oellermann, M. *et al.* Open Hardware in Science: The Benefits of Open Electronics. *Integr. Comp. Biol.* **62**, 1061–1075 (2022).
11. Chan, K. *et al.* Low-cost electronic sensors for environmental research: Pitfalls and opportunities. *Prog. Phys. Geogr. Earth Environ.* **45**, 305–338 (2021).
12. Eidam, E. F., Langhorst, T., Goldstein, E. B. & McLean, M. OpenOBS: Open-source, low-cost optical backscatter sensors for water quality and sediment-transport research. *Limnol. Oceanogr. Methods* **20**, 46–59 (2021).
13. Cory, R. M., Crump, B. C., Dobkowski, J. A. & Kling, G. W. Surface exposure to sunlight stimulates CO2 release from permafrost soil carbon in the Arctic. *Proc. Natl. Acad. Sci.* **110**, 3429–3434 (2013).
14. Ferrari, M. C. O., Lysak, K. R. & Chivers, D. P. Turbidity as an ecological constraint on learned predator recognition and generalization in a prey fish. *Anim. Behav.* **79**, 515–519 (2010).
15. Downing, J. Twenty-five years with OBS sensors: The good, the bad, and the ugly. *Cont. Shelf Res.* **26**, 2299–2318 (2006).
16. Matos, T. *et al.* Development of a Cost-Effective Optical Sensor for Continuous Monitoring of Turbidity and Suspended Particulate Matter in Marine Environment. *Sensors* **19**, 4439 (2019).
17. Trevathan, J., Read, W. & Schmidtke, S. Towards the Development of an Affordable and Practical Light Attenuation Turbidity Sensor for Remote Near Real-Time Aquatic Monitoring. *Sensors* **20**, 1993 (2020).
18. Jiang, H., Hu, Y., Yang, H., Wang, Y. & Ye, S. A Highly Sensitive Deep-Sea In-Situ Turbidity Sensor With Spectrum Optimization Modulation-Demodulation Method. *IEEE Sens. J.* **20**, 6441–6449 (2020).
19. Murphy, K. *et al.* A low-cost autonomous optical sensor for water quality monitoring. *Talanta* (2014) doi:10.1016/j.talanta.2014.09.045.
20. Kelley, C. D. *et al.* An Affordable Open-Source Turbidimeter. *Sensors* **14**, 7142–7155 (2014).
21. Kirkey, W. D., Bonner, J. S. & Fuller, C. B. Low-Cost Submersible Turbidity Sensors Using Low-Frequency Source Light Modulation. *IEEE Sens. J.* **18**, 9151–9162 (2018).
22. Kinar, N. J. & Brinkmann, M. Development of a sensor and measurement platform for water quality observations: design, sensor integration, 3D printing, and open-source hardware. *Environ. Monit. Assess.* **194**, 207 (2022).
23. Droujko, J. & Molnar, P. Open-source, low-cost, in-situ turbidity sensor for river network monitoring. *Sci. Rep.* **12**, 10341 (2022).
24. Sanchez, R., Groc, M., Vuillemin, R., Pujo-Pay, M. & Raimbault, V. Development of a Frugal, In Situ Sensor Implementing a Ratiometric Method for Continuous Monitoring of Turbidity in Natural Waters. *Sensors* **23**, 1897 (2023).
25. Droujko, J., Kunz Jr, F. & Molnar, P. Ötz-T: 3D-printed open-source turbidity sensor with Arduino shield for suspended sediment monitoring. *HardwareX* **13**, e00395 (2023).

26. Beddows, P. A. & Mallon, E. K. Cave Pearl Data Logger: A Flexible Arduino-Based Logging Platform for Long-Term Monitoring in Harsh Environments. *Sensors* **18**, 530 (2018).
27. Lyman, T. P., Elsmore, K., Gaylord, B., Byrnes, J. E. K. & Miller, L. P. Open Wave Height Logger: An open source pressure sensor data logger for wave measurement. *Limnol. Oceanogr. Methods* **18**, 335–345 (2020).
28. Temple, N. A., Webb, B. M., Sparks, E. L. & Linhoss, A. C. Low-Cost Pressure Gauges for Measuring Water Waves. *J. Coast. Res.* **36**, 661–667 (2020).
29. Thaler, A., Sturdivant, S. K., Neches, R. & Black, I. Openctd: Construction and Operation. (2020).
30. Favaro, E. A. & Lamoureux, S. F. Downstream patterns of suspended sediment transport in a High Arctic river influenced by permafrost disturbance and recent climate change. *Geomorphology* **246**, 359–369 (2015).
31. Tananaev, N. Hysteresis effects of suspended sediment transport in relation to geomorphic conditions and dominant sediment sources in medium and large rivers of Russian Arctic. *Hydrol. Res.* **46**, 232–243 (2015).
32. Mucking in the Marshes. *Endeavors* https://endeavors.unc.edu/mucking-in-the-marshes/ (2022).
33. Davies-Colley, R., Hughes, A. O., Vincent, A. G. & Heubeck, S. Weak numerical comparability of ISO-7027-compliant nephelometers. Ramifications for turbidity measurement applications. *Hydrol. Process.* **35**, e14399 (2021).
34. Snazelle, T. T. *Field Comparison of Five In Situ Turbidity Sensors*. https://doi.org/10.3133/ofr20201123. (2020).

Figures

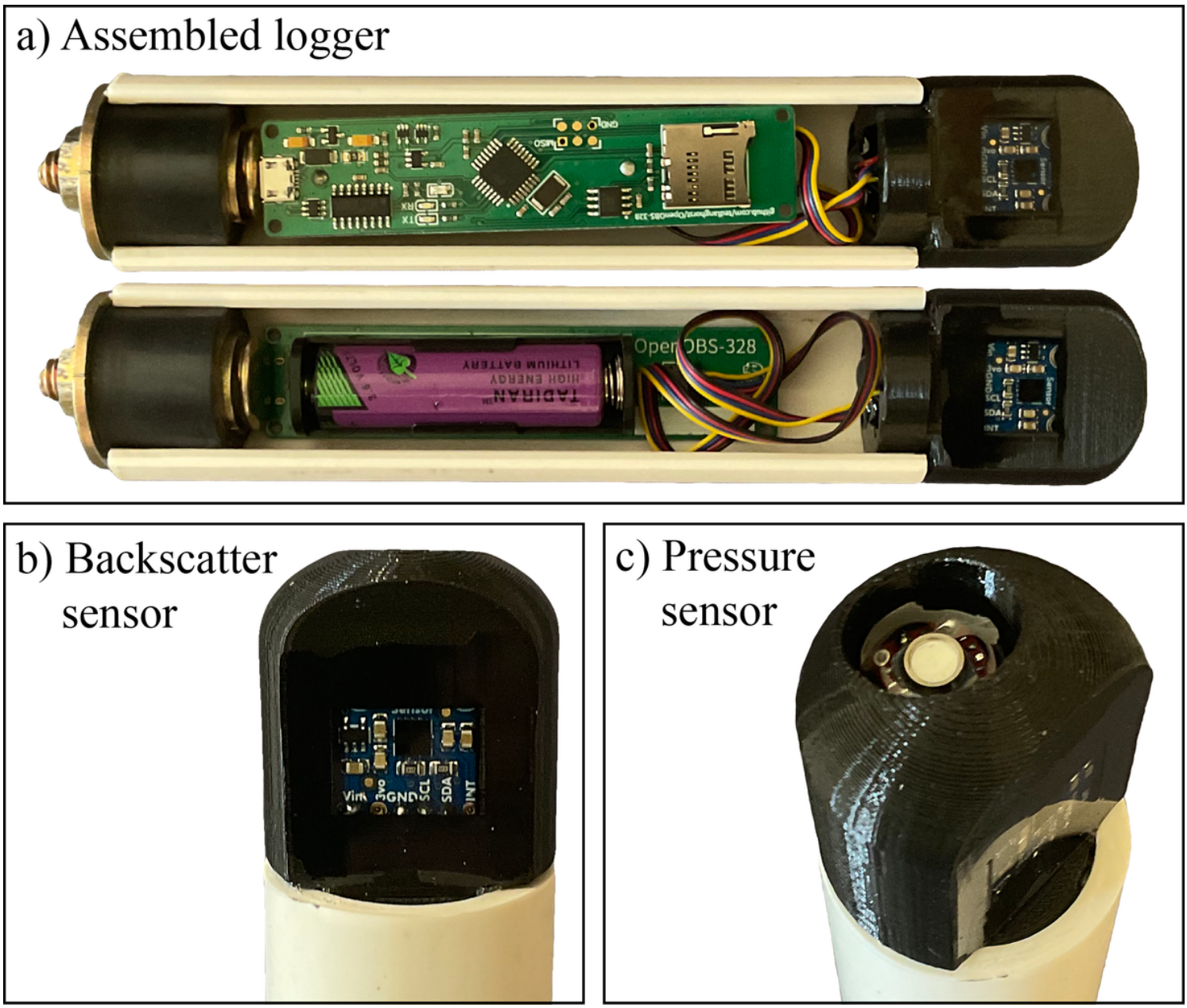

Figure 1

a) The fully assembled OpenOBS-328 logger (with housing cut open for visualization). b) MS5803 pressure sensor in the sensor head. The epoxy covers everything except the white pressure membrane. c) VCNL4010 proximity sensor for turbidity measurements.

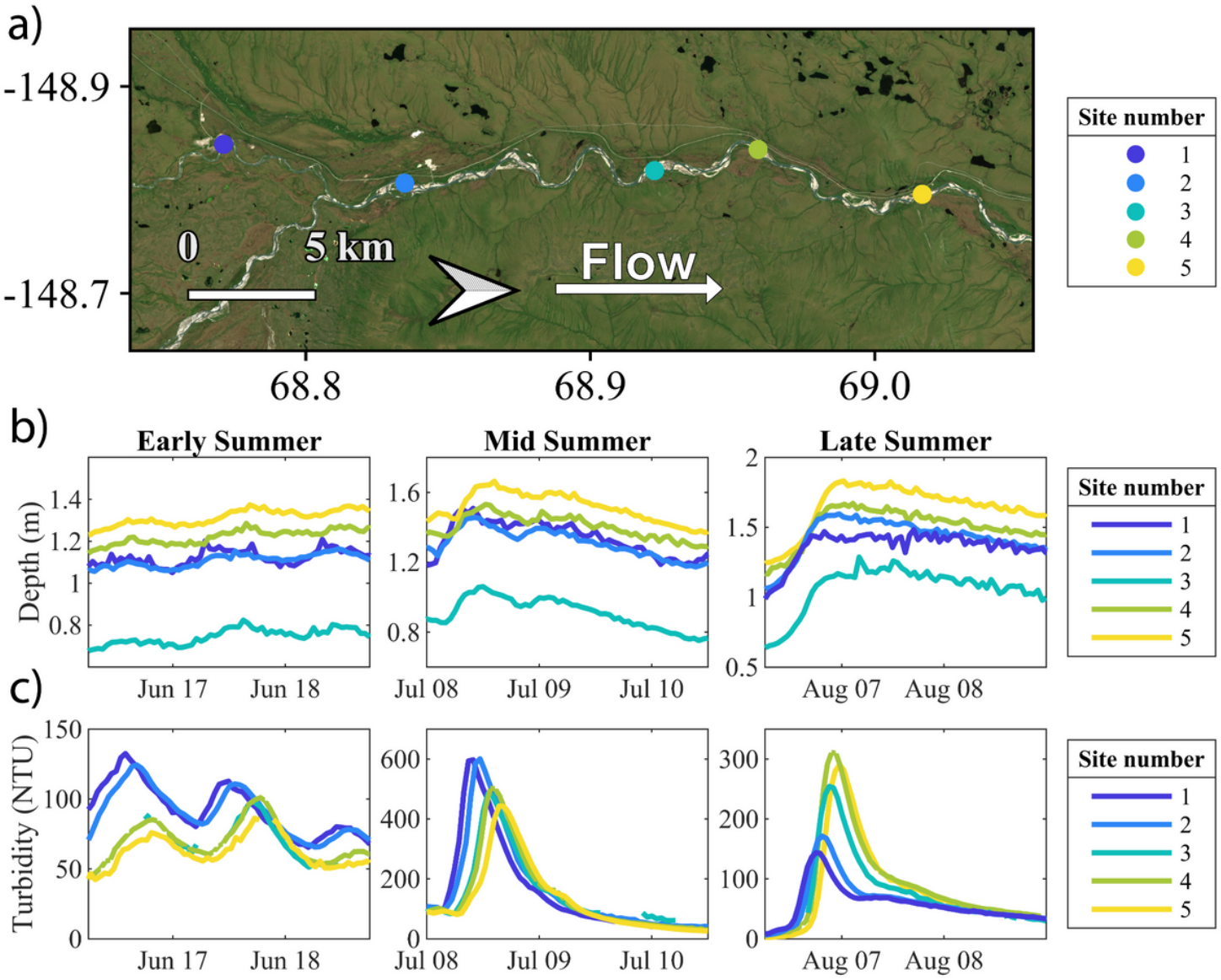

Figure 2

a) study area map of the Sagavanirktok River with the 5 instrumented sites plotted. b) and c) time series of depth turbidity at our 5 stations along the Sagavanirktok River. The three columns represent three periods over the summer of 2022. Note that the axis limits change from plot to plot for visibility.

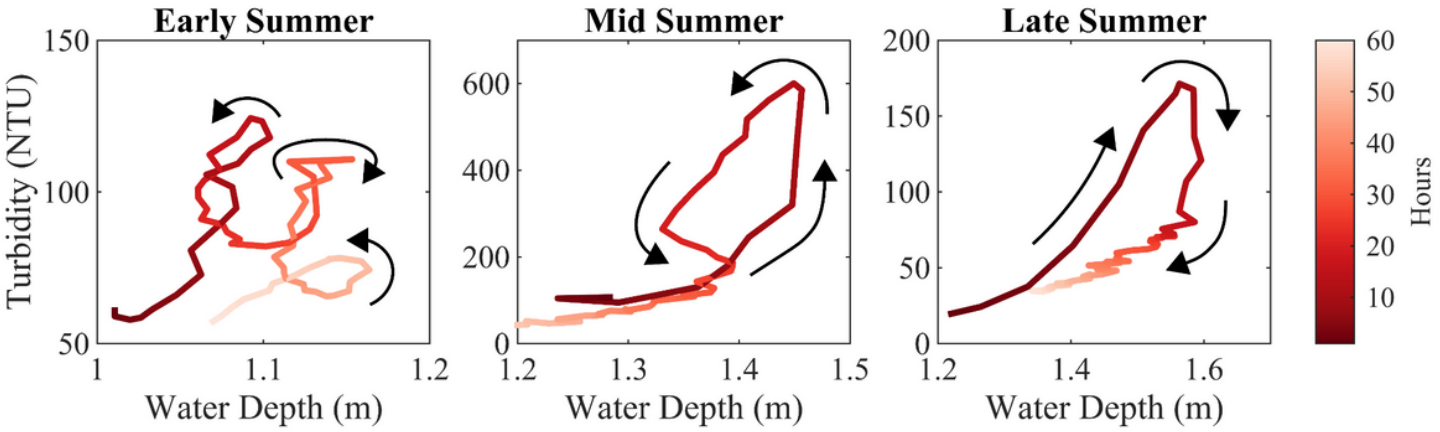

Figure 3

Hysteresis plots for three periods on the Sagavanirktok River. The data are from site two in Figure 2. Note that the axis limits change from plot to plot for visibility.

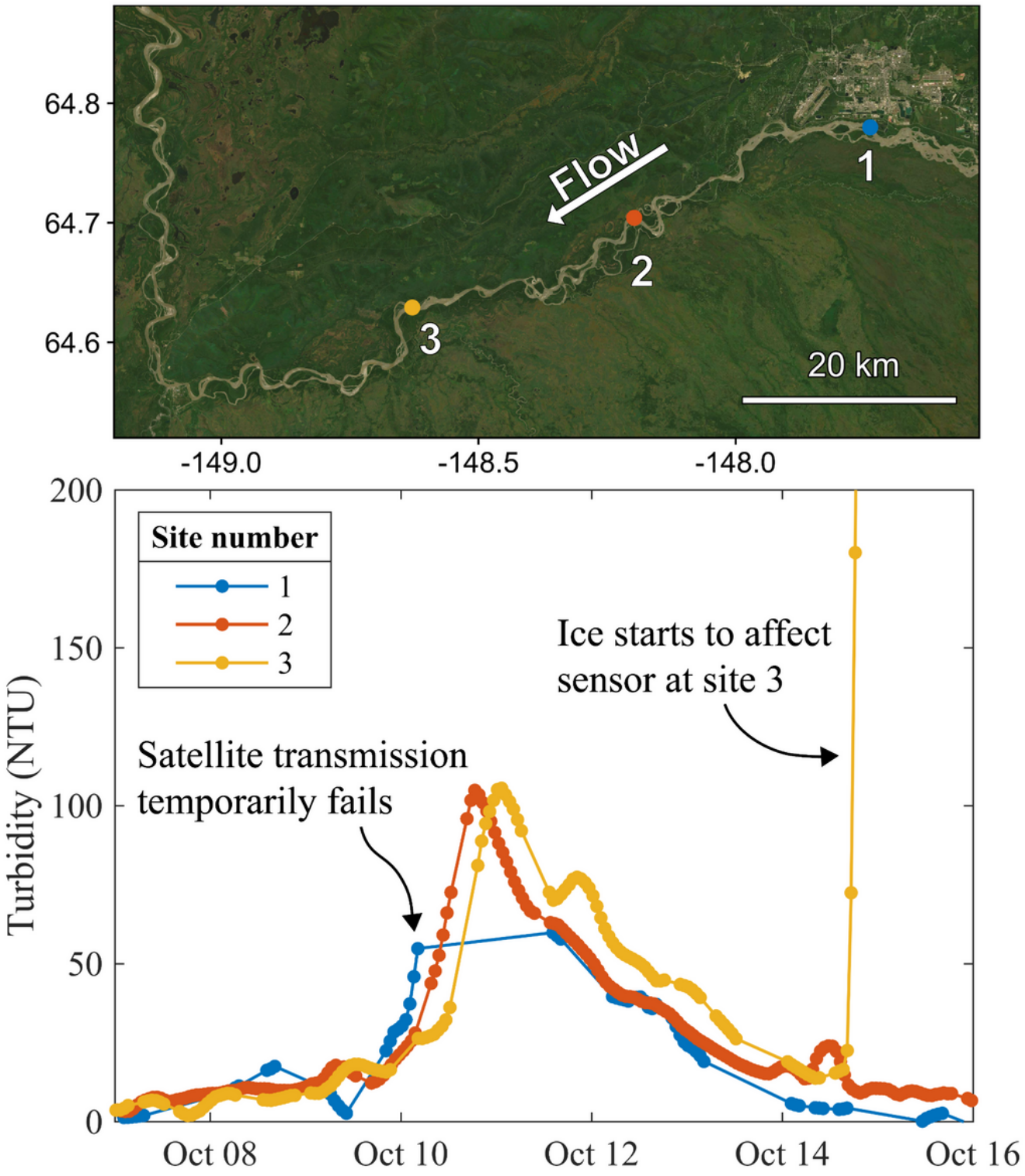

Figure 4

(top) Study area of the Tanana River, Alaska for the winter 2022/2023 logger installation. (bottom) Time series of Turbidity, showing a pulse of sediment that occurred shortly before freeze up. Points represent transmitted values, and the lines are interpolated. The sensor at site 3 was installed in fairly shallow water and started to be affected by ice before sensors at sites 1 and 2. The data not transmitted via

satellite from Site 1 from October 10-12 is stored on the SD card and can be used if we recover the logger after breakup.

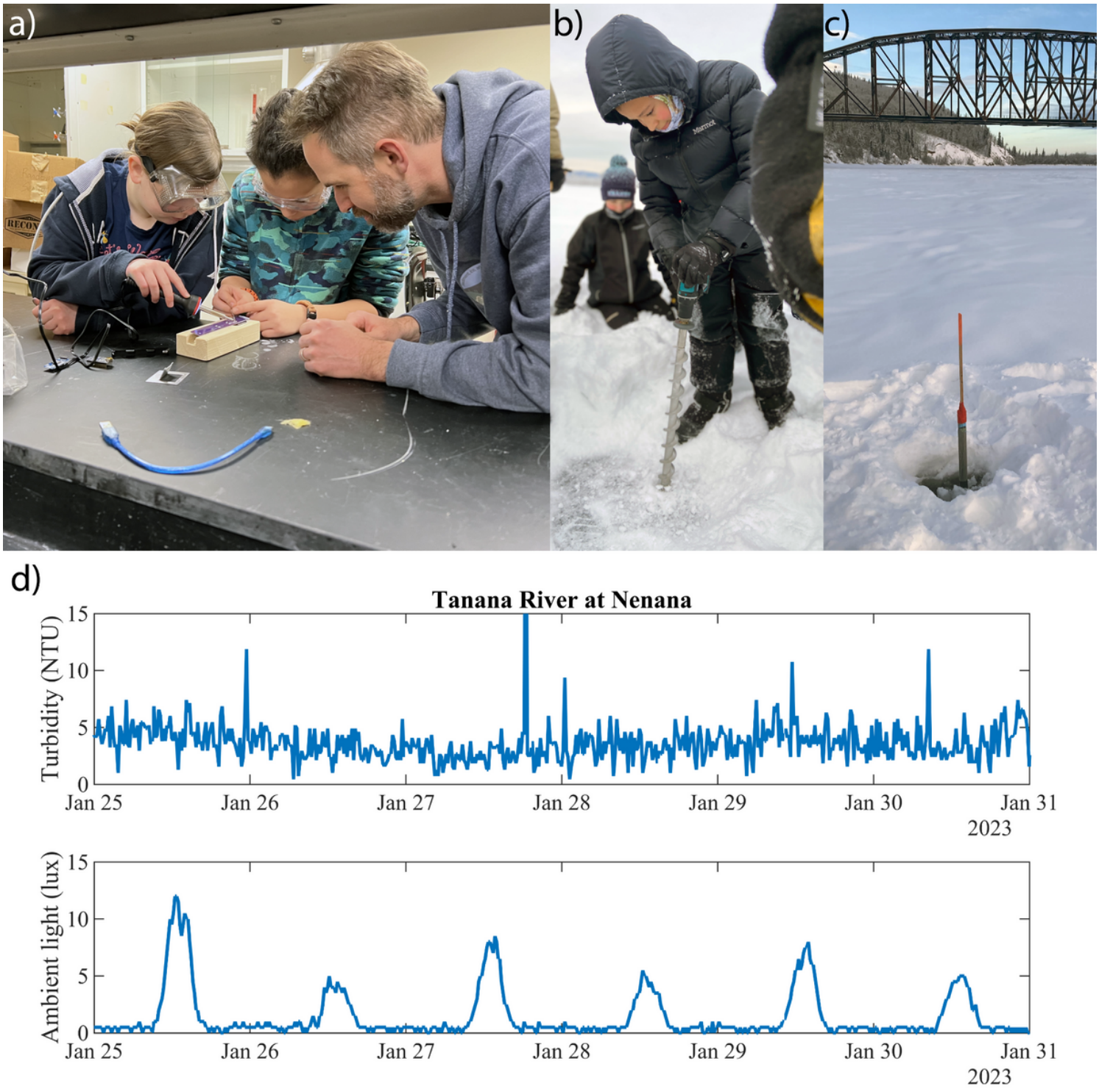

Figure 5

a) CyberLynx students and author TP soldering an OpenOBS at the University of Alaska Fairbanks campus. b) A CyberLynx student drilling into the ice on the Tanana River to install a sensor. c) one of four

student sensors installed in the Tanana River. d) Turbidity and Ambient light data from the sensor in panel c.

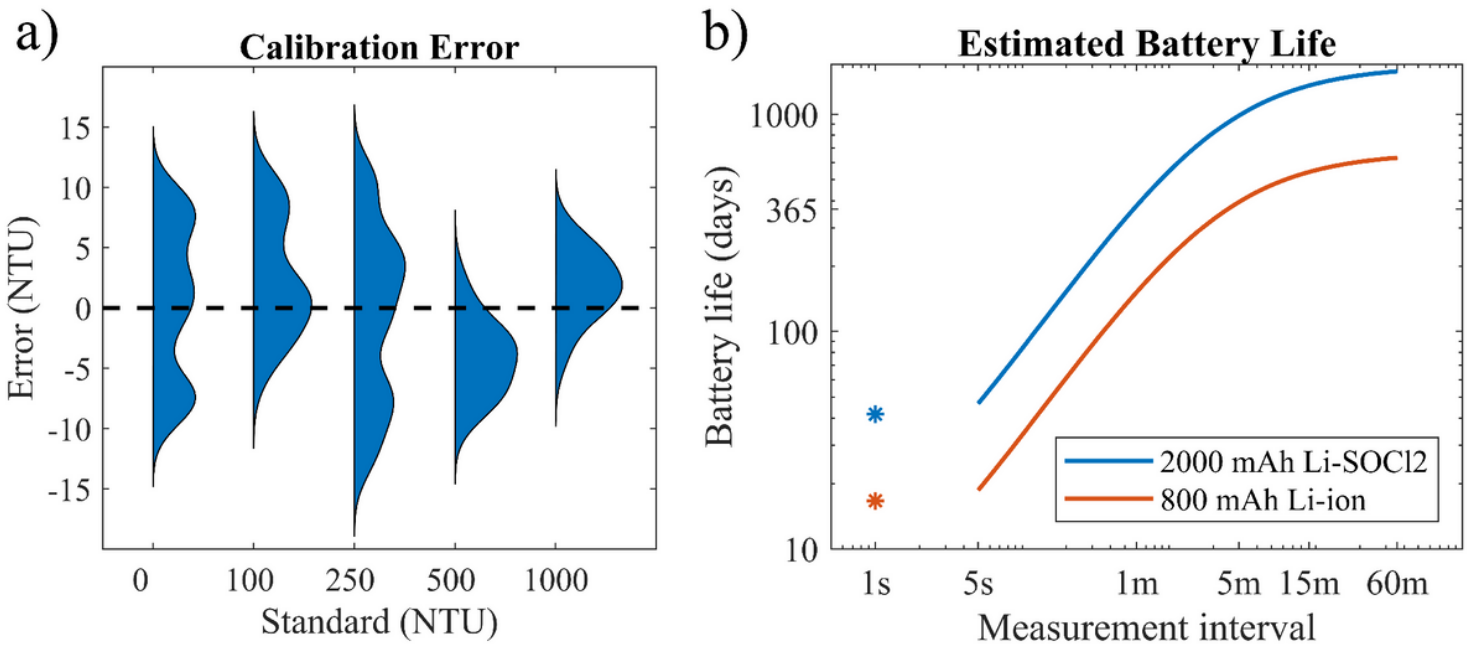

Figure 6

a) Distribution of calibration error based on the first 20 OpenOBS-328 sensors. b) Estimated battery life for non-rechargeable Lithium Thionyl Chloride (Li-SOCl2) and rechargeable Lithium-Ion (Li-ion) AA size batteries. The points marked by an asterisk for each battery represent continuous mode at 1 Hz and the lines represent measurement intervals greater than 5 seconds with low-power sleep between measurements.

Supplementary Files

This is a list of supplementary files associated with this preprint. Click to download.

- OpenOBS328Supplemental.docx